

# Application of BDD thin film electrode for electrochemical decomposition of heterogeneous aromatic compounds

Research Article

Justyna Czupryniak<sup>1</sup>, Aleksandra Fabiańska<sup>1</sup>, Piotr Stepnowski<sup>1</sup>, Tadeusz Ossowski<sup>1</sup>, Robert Bogdanowicz<sup>2\*</sup>, Marcin Gnyba<sup>2</sup>, Ewa M. Siedlecka<sup>1</sup>

<sup>1</sup> Analytical Chemistry, Faculty of Chemistry, University of Gdańsk  
18 Sobieskiego Str., 80-952 Gdańsk, Poland

<sup>2</sup> Department of Metrology and Optoelectronics, Gdańsk University of Technology,  
11/12 Narutowicza Str., 80-233 Gdańsk, Poland

Received 09 February 2012; accepted 05 April 2012

## Abstract:

The aim of the presented study is to investigate the applicability of electrochemical oxidation of aromatic compounds containing heteroatoms, e.g. waste from production of pesticides or pharmaceuticals, at a boron-doped diamond (BDD) electrode. The BDD electrodes were synthesized by microwave plasma enhanced chemical vapour deposition (MW PE CVD). Investigation of the electrode surface by optical microscopy and scanning electron microscopy (SEM) confirmed that the synthesized layer was continuous and formed a densely packed grain structure with an average roughness of less than 0.5  $\mu\text{m}$ . The influence of important electrochemical parameters: current density, kind of reactor, pH or mixing operation, on the efficiency of the oxidation was investigated. The fouling of electrode's surface caused by the deposition of organic material was observed during CV and galvanostatic experiments. At low current density the oxidation rate constant  $k$  was low, but the current efficiency was relatively high. The BDD can be used successfully to remove heterogeneous aromatic compounds existing either as molecules or cations. During 4 h of electrolysis 95% of aromatic compounds were electrochemically decomposed to mineral forms. It was observed that the influence of the initial pH on mineralization was marginal.

**PACS (2008):** 81.15.Gh, 82.45.Fk, 81.16.Pr, 82.45.Wx

**Keywords:** microwave plasma chemical vapour deposition • boron-doped diamond electrode • electrochemical oxidation • aromatic compounds

© Versita sp. z o.o.

## 1. Introduction

Waste products from pharmaceutical, textile and other chemical industries contain large amounts of non-biodegradable pollutants which must be treated before water discharge [1, 2]. However, recently used treat-

\*E-mail: rbogdan@eti.pg.gda.pl (Corresponding author)

ments such as adsorption, coagulation or chemical oxidation by ozone are not sufficient for efficient waste removal and therefore the application of advanced oxidation processes (AOPs) to the degradation of toxic or non-biodegradable organic pollutants has been widely investigated [3]. Chemical (Fenton, Fenton-like), photochemical (photo-Fenton, UV/TiO<sub>2</sub>, UV/H<sub>2</sub>O<sub>2</sub>/UV), and sonochemical (H<sub>2</sub>O<sub>2</sub>/CH<sub>3</sub>COOH/sonication) advanced oxidation processes are very potent in oxidization, decolorization, and degradation of anthropogenic compounds. AOPs are designed to generate hydroxyl radicals (one of the strongest oxidants) as a primary and non-selective oxidizing agent. However, they are still not economical processes for wastewater treatment due to their high operating cost, reduction of efficiency by turbidity, deactivation of the catalyst, relatively poor mineralization, low pH necessary for carrying out Fenton process etc. Electrochemical processes are more promising and allow the above mentioned drawbacks to be avoided. Electrochemical conversion and combustion seem to be environmentally friendly, because the only reagent used is electrical current, pH is neutral and mineralization is more extended than, for example, in the Fenton process. In general, electrodes for the oxidation of organic pollutants can be made from numerous materials [4–7]. However, for wide application of electrochemical degradation it is necessary to optimize electrolysis conditions, e.g. by ensuring desirable properties of the electrode materials: high stability, high activity and low cost. The main attention of researchers worldwide is focused on so called “non-active” anodes such as boron doped diamond (BDD). They have good chemical and electrochemical stability even in highly aggressive media, long lifetime and a wide potential window for water discharge. In classical anode materials (Pt or C) transfer reactions of oxygen are slow and have low Faradaic yields. The utilization of anodes with high oxygen overpotential, e.g. BDD electrodes, enhances the compounds degradation and increases the current efficiency [8, 9]. The use of BDD thin film electrodes in anodic oxidation has shown that O<sub>2</sub> overvoltage is much higher than for conventional anodes, such as PbO<sub>2</sub>, producing larger amounts of quasi-free OH radicals and other oxidants (depending on supporting electrolytes). Oxidation of pollutants at these anodes produces CO<sub>2</sub> and H<sub>2</sub>O via a sequence of chemical reactions [10, 11]. Another important advantage of the BDD electrodes is their stability under polarity inversion [12]. The important properties for BDD electrodes for industrial applications, including their lifetime and cost, are significantly determined by their manufacturing process [9]. Organic pollutants on BDD electrodes can be oxidized directly (by electron transfer from surface to compound) and indirectly (by oxidizing entities

generated on the electrode surface by electrolysis of water) [2]. It has also been demonstrated that other biorefractory compounds such as pesticides, pharmaceuticals and dyes can be completely mineralized with high current efficiency [13–15]. Electrochemical study was performed to achieve and optimize the parameters of this process. Evaluation of the quality of BDD electrodes was achieved by investigation of the surface of the deposited diamond layers and studying layer thickness and surface morphology. Electrochemical experiments were also performed using deposited BDD layers and Cyclic voltammograms were measured in water solution in the positive region of potential related to the reference electrode. To monitor the progress of aromatic compound degradation, samples were taken at appropriate time intervals and the concentrations of the compounds were measured by HPLC-UV.

## 2. Experimental

### 2.1. BDD electrodes synthesis

The BDD electrodes were synthesized in a custom-made PE CVD system on highly doped single-crystal p-type Si <100> substrates. They were pre-treated by diamond nanopowder with an average granulation of 5 nm to increase diamond nucleation. Substrate temperature was kept at 800°C during deposition process. Highly excited plasma was ignited by microwave radiation (2.45 GHz) in the electron resonance conditions [16, 17]. The plasma microwave power, optimized for diamond synthesis [18], was kept at 1500 W. The molar ratio of CH<sub>4</sub> - H<sub>2</sub> mixture was kept at 1% of gas volume and at 100 sccm of total flow rate. The base pressure was about 10<sup>-5</sup> Pa and the process pressure was kept at 13 Pa. The doping level of boron in the diamond layer, expressed as the B/C ratio, was about 4000 ppm. The resistivity of the resulting doped diamond film was in the range of 10–30 mΩ cm. Electrodes were investigated using spectroscopic ellipsometry carried out with a phase modulated ellipsometer (Jobin-Yvon UVISSEL, HORIBA Jobin-Yvon Inc., Edison, USA). The ellipsometric angles Δ and Ψ were measured at an incident angle of 70° to the silicon substrate in the wavelength range 400–700 nm. The thickness of the films were determined by fitting the ellipsometric data to a Tauc-Lorentz model [19–21]. Surface morphology analysis was performed using high resolution optical microscopy (Leica Reichert MEF4M with 1000× magnification) and scanning electron microscopy (Philips-FEI XL 30 ESEM with 4000× magnification).

## 2.2. Electrochemical setup

Electrochemical experiments were performed using a glass container with a working volume of 85 ml, placed in thermoregulated water bath attached with a magnetic stirrer. The electrolysis experiments were conducted at a constant temperature of  $25 \pm 1^\circ\text{C}$  using a potentiostat/galvanostat system (PGSTAT-30 Autolab). A BDD/stainless steel electrode with an effective surface area of  $9.25\text{ cm}^2$  (for CV) and  $25.5\text{ cm}^2$  (for galvanostatic experiments) was used as working electrode. A standard reference electrode of Ag/AgCl and a Pt counter electrode were utilized with the area of the counter electrode equal to the area of working BDD electrode. Both BDD and stainless steel electrodes were square type plates with an inter-electrode gap of 1 cm. Cyclic voltammograms were measured in unstirred solution with a computer controlled system. Prior to every experimental run, the working BDD electrode was polarized anodically for 5 min in  $0.5\text{ M H}_2\text{SO}_4$  electrolyte solution with a constant current of 100 mA while the stainless steel cathode was soaked in  $0.5\text{ M H}_2\text{SO}_4$  for 10 min to remove any kind of deposition and/or impurities from the surface. Some electrochemical decomposition experiments were carried out in a double compartment electrolysis cell equipped with a Nafion anion exchange membrane. Furthermore, chemical oxygen demand (COD) was measured after 4 h of electrolysis by using cuvette tests and an Odyssey spectrophotometer (Hach, USA). The pH was measured by a pH-meter 330i (WTW GmbH, Germany). For the determination of the electrochemical degradation studies a HPLC (VWR Hitachi, Japan) system "LaChrome Elite" was used, containing a L-2130 HTA-pump, L-2130 degasser, L-2350 column oven, L-2450 diode array-detector and EZ Chrome Elite software. A cation exchanger (CC 125/4 Nucleosil 100-5SA) with a guard column was employed. The mobile phase consisted of 55% acetonitrile and 45% aqueous solution of 25 mM  $\text{KH}_2\text{PO}_4$  and 3.2 mM  $\text{H}_3\text{PO}_4$ . The system was operated at a flow rate of 1 ml/min and 10  $\mu\text{l}$  portions of the samples were injected. A two detection wavelengths of 212 nm and 254 nm were respectively used for quantification of ILs and sulfametoxazole.

## 3. Results and discussion

### 3.1. Electrode surface analysis

The surface analysis was performed using high-resolution optical microscopy and scanning electron microscopy (see Fig. 1). The SEM analysis of the electrode surface showed that the doped diamond layer was continuous with crystalline clusters of about 500 nm across. Such a small

crystal size enables higher surface area and increases the amount of active sites where electrochemical reactions could be carried out [22]. The closed film surface prevents the substrate influencing with the electrochemical system.

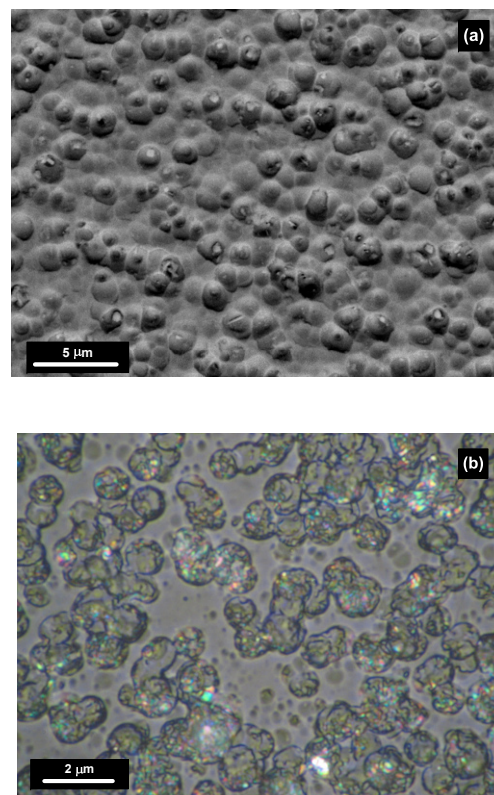


**Figure 1.** Pictures of diamond layer taken by: (a) scanning electron microscopy with  $4000\times$  magnification, (b) optical microscopy with  $1000\times$  of magnification.

Optical microscopy (Fig. 1b) shows that samples are visually smooth, flat and transparent. The synthesized layer forms a densely packed grain structure and the roughness is less than 0.5 micron. Visible grains and pores could be observed in microscopic images. The average diamond layer thickness, investigated by spectroscopic ellipsometry, was  $2\text{ }\mu\text{m}$  which is four times more than roughness extracted from SEM investigations. Such a result proves that whole area of surface is closed and electrochemically active.

### 3.2. Parameters of organic compound degradation

The BDD was used as an anode in the electrolyser for ionic liquid (1-butyl-3-methylimidazolium chloride) and

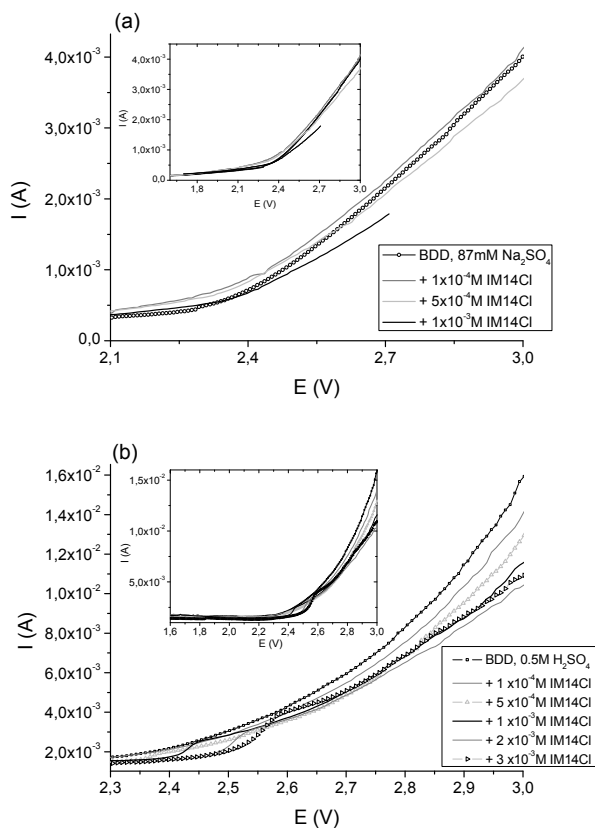


**Figure 2.** Cyclic voltammograms on BDD anode for 0.1–10 mM of 1-butyl-3-methylimidazolium cation in 0.087 M of  $\text{Na}_2\text{SO}_4$  (a) and 0.5 M  $\text{H}_2\text{SO}_4$  (b) electrolytes.

drug (sulfamethoxazole) decay. Previously, cyclic voltammetry experiments were carried out to obtain information about the redox response of 1-butyl-3-methylimidazolium chloride (IM14Cl) [23, 24]. In Fig. 2 cyclic voltammograms of a BDD electrode with various aqueous solutions containing from 0.1 mM to 10 mM of IM14Cl in 0.087 M of  $\text{Na}_2\text{SO}_4$  and 0.5 M  $\text{H}_2\text{SO}_4$  as a supporting electrolyte are shown. The curves were obtained with a scan rate of  $100 \text{ mV s}^{-1}$  in the potential region from 1.6 V up to 3.0 V (vs. AgCl/Ag electrode). A cyclic voltammogram without organic matter is also plotted in the graphs for the sake of comparison. As can be observed, the presence of organic matter leads to the shift of oxygen evolution current to more positive potentials in both electrolytes. This can be explained by some sort of deactivation of the anode surface after the oxidation of IM14Cl which reduces the extension of the water oxidation to hydrogen radicals. Fouling was also observed during galvanostatic electrolysis and the cell potential increased in range 0.05–0.1 V over a period of 4 h.

The complete mineralization of organic matter at the BDD anode was only obtained at properly chosen operating parameters such as current density, supporting electrolyte, temperature, pH etc. Therefore, the degradation of IM14Cl was performed by galvanostatic electrolysis under different experimental conditions. Current density was an important parameter for organic compound removal. As presented in Fig. 3, changing current density clearly influenced the cumulative current efficiency ( $CE$ ) and oxidation rate constant  $k$ . The cumulative current efficiency of electrolysis is defined by relationship (1) [25]:

$$CE = \frac{[COD_0 - COD_t]}{8I\Delta t} FV \quad (1)$$

where  $COD_0$  and  $COD_t$  ( $\text{g O}_2 \text{ m}^{-3}$ ) correspond to concentration at  $t=0$  and  $t=t(\text{s})$  respectively,  $I$  is the applied current (A),  $F$  is the Faraday constant ( $96487 \text{ C/mol}$ ),  $V$  is the liquid holdup (L) and 8 is the equivalent mass of oxygen ( $\text{g/eq}$ ). At low current density the oxidation rate constant  $k$  is low but the current efficiency is relatively high. The increase of current density from  $8 \text{ mA/cm}^2$  to  $24 \text{ mA/cm}^2$  decreases the current efficiency from 61% to 23%. This indicates that the process is under mass control and the increase of current density wastes the electrical energy through an oxygen evolution side reaction. At the lowest current density the imidazolium cation was completely eliminated in about 2 h and 95%  $COD$  removal was achieved after 4 h of electrolysis.

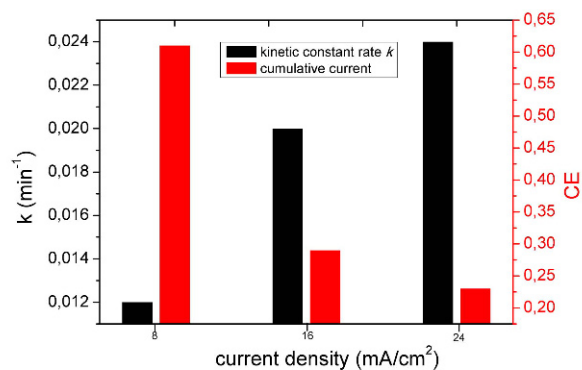


**Figure 3.** The influence of current density on pseudo-first kinetic constant rate  $k$  and cumulative current efficiency ( $CE$ ) of 1-butyl-3-methylimidazolium cation removal at BDD anode. (0.087 M  $\text{Na}_2\text{SO}_4$  was electrolyte,  $\text{pH} = 6.5$ ).

The results obtained in single and double compartment reactor are shown at Fig. 4. The data indicates that the removal of organic matter was more rapid in the reactor with separate anode and cathode space. The elimination of imidazolium cation was observed only in the anode

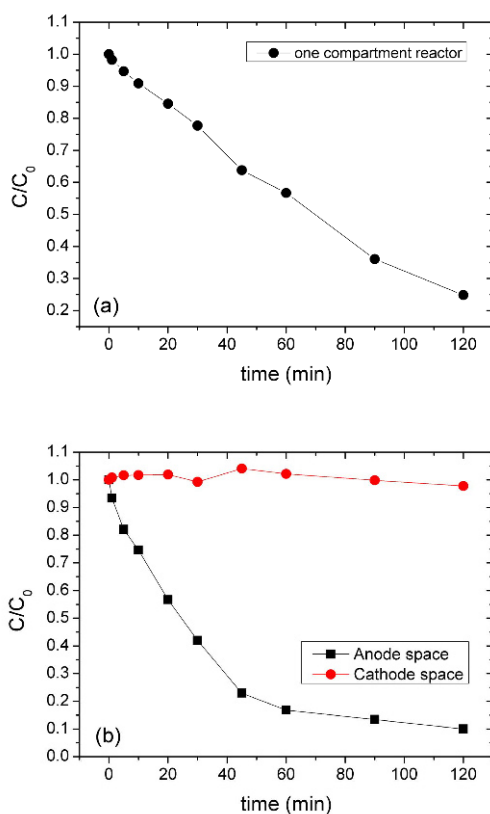


**Figure 4.** 1-butyl-3-methylimidazolium cation degradation in single (a) and double (b) compartment reactor with BDD anode and stainless steel cathode at current density  $16 \text{ mA cm}^{-2}$ .

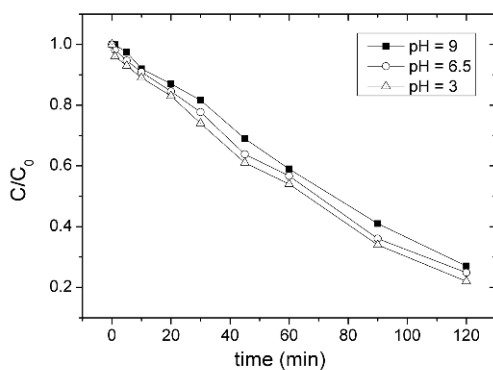


**Figure 5.** The role of initial pH on the oxidation of IM14Cl at BDD anode.

space, where the direct production of hydroxyl radicals ( $\text{OH}\bullet$ ) from aqueous electrolysis takes a part [26]. This indicates that the parent compound is removed from water only by oxidation. The oxidation trend of  $\text{IM14}^+$  at the anode suggests that it is initially current controlled

and becomes diffusion controlled at the end of the reaction when the concentration of  $\text{IM14}^+$  is very low. In contrast to this, the oxidation rate in single compartment reactor is lower. This fact is connected with lower concentration of ( $\text{OH}\bullet$ ) radicals caused by the increase in the volume of the reactor that exhibited oxidation. A reduction of intermediates at the cathode is also possible. Additionally, the mixing operation influenced the oxidation rate.

The role of initial pH on the oxidation of  $\text{IM14Cl}$  at the BDD surface was also studied. It was observed that the influence of initial pH (3.0, 6.5 and 9.0) on mineralization is marginal, as presented in Fig. 5. In this case, the acidic condition is slightly favorable because of the highly reactive nature of ( $\text{OH}\bullet$ ) and  $\text{S}_2\text{O}_8^{2-}$  [27, 28]. However, during electrolysis the pH of the aqueous solution was found to shift towards acidic which probably caused similar conditions in all experiments after some period of time. This acid pH may be due to the formation of carboxylic acids as an oxidation intermediate.

### 3.3. Degradation of heterogeneous organic compounds

Comparative study of the decomposition of two imidazolium compounds at the BDD anode was carried out (see Fig. 6). The results obtained indicate that N-substitution of the butyl alkyl side chain to methylimidazole caused a decrease of oxidation rate.

Our previous investigations showed that oxidation rate of imidazolium IIs decreased with the lengthening of alkyl side chain in imidazolium cation in other Advanced Oxidation Processes [23, 24, 29]. In these AOPs the main oxidants were hydroxyl radicals, which also played the main role in oxidation of imidazolium cation at the BDD anode<sup>1</sup>.

A possible pathway of imidazolium cation electrodegradation is presented in Fig. 7. During electrolysis the oxidative cleavage of the imidazolium ring led to mineral products such as ammonium, nitrate ions and small molecular organic compounds with carbonyl or carboxylic groups in structure. It can be observed in Fig. 8 that the concentration of  $\text{NH}_4^+$  and  $\text{NO}_3^-$  increased with the electrolysis time. The amount of  $\text{NO}_3^-$  was similar for both organic compound mixtures, but the amount of  $\text{NH}_4^+$  was higher for  $\text{IM1}^+$  than for  $\text{IM14}^+$  mixture. These results suggest that mineralization of  $\text{IM1}^+$  was more extended. During electrolysis 90% and 80% of imidazolium rings were mineralized for  $\text{IM1}^+$  and  $\text{IM14}^+$  respectively.

<sup>1</sup> E. M. Siedlecka et al., *J. Hazard. Mater.* (submitted)

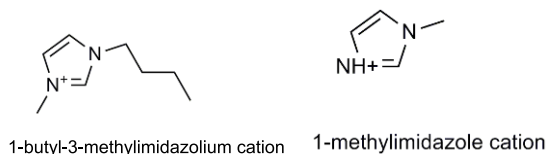
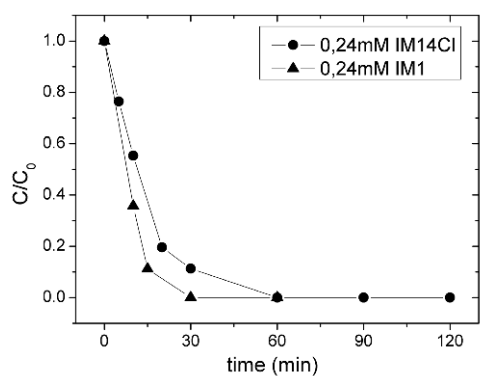


**Figure 6.** The electrooxidation of 1-butyl-3-methylimidazolium chloride (IM14Cl) and 1-methylimidazole (IM1) at BDD anode. Experimental conditions: 87 mM Na<sub>2</sub>SO<sub>4</sub>, pH = 6.5, U = 2.5V, surface of anode (BDD) and cathode (stainless steel) - 25.5 cm<sup>2</sup>.

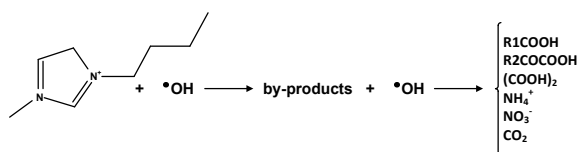


**Figure 7.** A possible pathway of imidazolium cation electrodegradation.

The results of electrochemical oxidation of sulfamethoxazole are shown in Fig. 9 and a detailed list of the main by-products are identified in Fig. 10. They are: p-benzoquinone, NH<sub>4</sub><sup>+</sup>, NO<sub>3</sub><sup>-</sup> and SO<sub>4</sub><sup>2-</sup>. Complete degradation of sulfamethoxazole was achieved after 4 h. Moreover, total mineralization of parent compound and by-products to CO<sub>2</sub> was found after 5 h of electrolysis. The reaction pathway for the mineralization of sulfamethoxazole is based on the identified by-products and suggests a few steps: hydroxylation of sulfamethoxazole on the sulfanilic ring and 3-amino-5-methylisoxazole, followed by the formation of p-benzoquinone from sulfanilic compound and its oxidative cleavage to the formation of carboxylic acids that were finally mineralized to CO<sub>2</sub>. 3-amino-5-methylisoxazole and sulfanilic acid released the NH<sub>4</sub><sup>+</sup>. Some NO<sub>3</sub><sup>-</sup> was observed as a result of NH<sub>4</sub><sup>+</sup> oxidation.

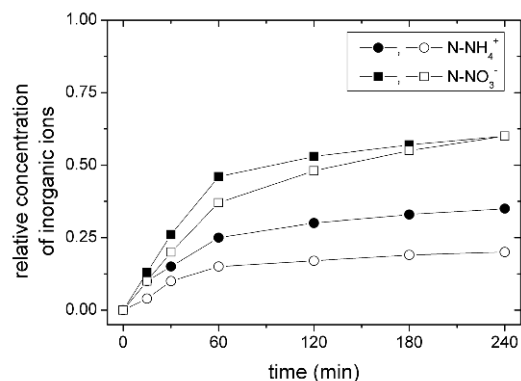


**Figure 8.** Time course of the relative concentration of the inorganic ions during the 1-methylimidazole (IM1) (■, ●) and 1-butyl-3-methylimidazolium chloride (IM14Cl) (□, ○) electrooxidation at BDD anode. Experimental conditions: 87 mM Na<sub>2</sub>SO<sub>4</sub>, pH = 6.5, U = 2.5V, surface of anode (BDD) and cathode (stainless steel) - 25.5 cm<sup>2</sup>.

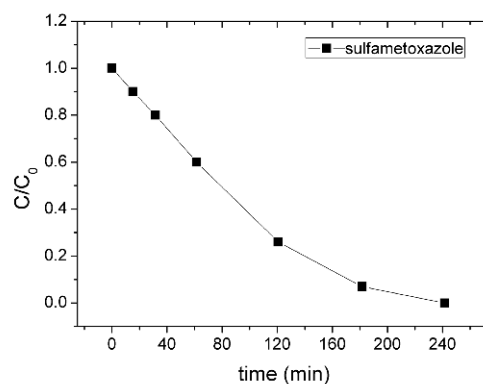


**Figure 9.** Electrochemical oxidation of sulfamethoxazole at BDD electrode (0.087 M Na<sub>2</sub>SO<sub>4</sub>, initial pH = 3).

## 4. Conclusions

The results of microscopic investigations confirm that the synthesized BDD film is continuous. It forms a densely packed grain structure with a roughness of less than 0.5 micron. Visible grains and pores could be observed in microscopic images. SEM images clearly show the progress of the BDD film nucleation, which exhibits polycrystalline structure. In the first phase independent grain-clusters are formed and they subsequently grow and expand in volume. In the final phase grains come into contact with each other building a continuous high density layer. The SEM analysis also showed that the size of the crystalline clusters was about 500 nm. Such a small crystal size enables higher surface area and increases the amount of active sites where electrochemical reactions

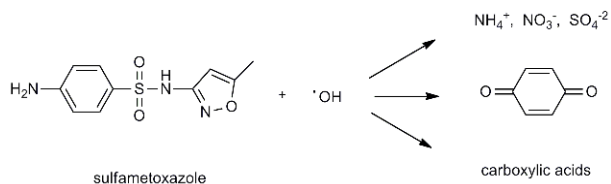


**Figure 10.** The main by-products of sulfamethoxazole oxidation at the BDD anode.

could be carried out. The BDD can be used successfully to remove heterogeneous aromatic compounds existing as either molecules or cations. During 4 h of electrolysis 95% of IM14<sup>+</sup> was electrochemically decomposed to mineral forms. The drug sulfamethoxazole decayed more rapidly. In cycle voltammetry experiments the fouling of the electrode's surface, caused by the deposition of organic material generated from IM14<sup>+</sup>, was observed. During 4 h of galvanostatic electrolysis the cell potential also increased in the range 0.05–0.1 V. Some operating parameters like current density, initial pH and reactor cell volume influence the rate and efficiency of the oxidation. The obtained data points out that increasing the current density caused the increase of IM14<sup>+</sup> oxidation rate but also the decrease of cumulative current efficiency. The marginal influence of initial pH on oxidation of IM14<sup>+</sup> was also observed. In all cases during electrolysis the pH dropped, indicating that part of the degraded molecules remained in aqueous solution probably as carboxylic acids. The obtained results showed that the BDD electrode is very useful for elimination of non-biodegradable and biological active compounds from water or wastewater, but for the total degradation of organic matter the proper oxidation parameters should be investigated and selected.

## Acknowledgments

This work was supported by MNiSzw project no. N N515 510 640 and N N523 42 3737 and by the NCBiR project LIDER/20/91/L-2/10. Further projects DS/ 8270-4-0093-12 and DS/ 8210-4-0177-1 and funds of Faculty of Electronics, Telecommunications and Informatics of the Gdansk University of Technology are also acknowledged.

## References

- [1] C. A. Martínez-Huitle, S. Ferro, *Chem. Soc. Rev.* 35, 1324 (2006)
- [2] C. Guohua, *Sep. Purif. Technol.* 38, 11 (2004)
- [3] M. Panizza, G. Cerisola, *Ind. Eng. Chem. Res.* 47, 6816 (2008)
- [4] I. Sirés, E. Brillas, G. Cerisola, M. Panizza, *J. Electroanal. Chem.* 613, 151 (2008)
- [5] E. Brillas, S. Garcia-Segura, M. Skoumal, C. Arias, *Chemosphere* 79, 605 (2010)
- [6] J. Iniesta, J. González-García, E. Expósito, V. Montiel, A. Aldaz, *Water Res.* 35, 3291 (2001)
- [7] S. K. Johnson, L. L. Houk, J. Feng, R. S. Houk, D. C. Johnson, *Environ. Sci. Technol.* 33, 2638 (1999)
- [8] M. Panizza, G. Cerisola, *Electrochim. Acta* 51, 191 (2005)
- [9] V. Schmalz, T. Dittmar, D. Haaken, E. Worch, *Water Res.* 43, 5260 (2009)
- [10] U. Griesbach, D. Zollinger, H. Pütter, C. Comninellis, *J. Appl. Electrochem.* 35, 1265 (2005)
- [11] A. Kapałka, G. Fóti, C. Comninellis, *J. Appl. Electrochem.* 38, 7 (2007)
- [12] T. Furuta et al., *Diam. Relat. Mat.* 13, 2016 (2004)
- [13] A. Morao, A. Lopes, M. T. Pessoa de Amorim, I. C. Gonçalves, *Electrochim. Acta* 49, 1587 (2004)
- [14] Y. Samet, L. Agengui, R. Abdelhédi, *Chem. Eng. J.* 161, 167 (2010)
- [15] E. Weiss, K. Groenen-Serrano, A. Savall, *J. Appl. Electrochem.* 38, 329 (2007)
- [16] R. Bogdanowicz, M. Gnyba, P. Wroczyński, B. B. Kosmowski, *J. Optoelectron. Adv. M.* 12, 1660 (2010)
- [17] R. Bogdanowicz, M. Gnyba, P. Wroczyński, *J. Phys. IV* 137, 57 (2006)
- [18] R. Bogdanowicz, *Acta Phys. Pol. A* 114, A33 (2008)
- [19] H. G. Tompkins, *A User's Guide to Ellipsometry* (Academic Press, 1993)
- [20] G. E. Jellison Jr. et al., *Thin Solid Films* 377–378, 68 (2000)
- [21] S. Boycheva, C. Popov, W. Kulisch, J. Bulir, A. Piegari, *Fullerenes, Nanotubes and Carbon Nanostructures* 13, 457 (2005)
- [22] I. Duo, C. Levy-Clement, A. Fujishima, C. Comninellis, *J. Appl. Electrochem.* 34, 935 (2004)
- [23] E. M. Siedlecka, P. Stepnowski, *Environ. Sci. Poll. Res.* 16, 453 (2008)
- [24] M. Czerwicka et al., *J. Hazard. Mater.* 171, 478 (2009)
- [25] C. A. Martínez-Huitle, M. A. Quiroz, C. Comninellis, S. Ferro, A. D. Battisti, *Electrochim. Acta* 50, 949 (2004)
- [26] C. Comninellis, *Electrochim. Acta* 39, 1857 (1994)
- [27] B. Marselli, J. Garcia-Gomez, P.-A. Michaud, M. A. Rodrigo, C. Comninellis, *J. Electrochem. Soc.* 150, D79 (2003)
- [28] P.-A. Michaud, E. Mahe, W. Haenni, A. Perret, C. Comninellis, *Electrochem. Solid-State Lett.* 3, 77 (2000)
- [29] E. M. Siedlecka et al., *Appl. Catal. B: Environ.* 91, 573 (2009)